MOLECULAR AND CELLULAR BIOLOGY, Mar. 2003, p. 2162–2170 Vol. 23, No. 6
0270-7306/03/$08.00+0 DOI: 10.1128/MCB.23.6.2162–2170.2003

Cortactin Is a Component of Clathrin-Coated Pits and Participates in Receptor-Mediated Endocytosis

Hong Cao,[1] James D. Orth,[1] Jing Chen,[1] Shaun G. Weller,[1] John E. Heuser,[2] and Mark A. McNiven[1]*

Department of Biochemistry and Molecular Biology, Mayo Clinic, Rochester, Minnesota 55905,[1] and Department of Cell Biology and Physiology, Washington University School of Medicine, St. Louis, Missouri 63130[2]

Received 7 June 2002/Returned for modification 3 July 2002/Accepted 6 December 2002

The actin cytoskeleton is believed to contribute to the formation of clathrin-coated pits, although the specific components that connect actin filaments with the endocytic machinery are unclear. Cortactin is an F-actin-associated protein, localizes within membrane ruffles in cultured cells, and is a direct binding partner of the large GTPase dynamin. This direct interaction with a component of the endocytic machinery suggests that cortactin may participate in one or several endocytic processes. Therefore, the goal of this study was to test whether cortactin associates with clathrin-coated pits and participates in receptor-mediated endocytosis. Morphological experiments with either anti-cortactin antibodies or expressed red fluorescence protein-tagged cortactin revealed a striking colocalization of cortactin and clathrin puncta at the ventral plasma membrane. Consistent with these observations, cells microinjected with these antibodies exhibited a marked decrease in the uptake of labeled transferrin and low-density lipoprotein while internalization of the fluid marker dextran was unchanged. Cells expressing the cortactin Src homology three domain also exhibited markedly reduced endocytosis. These findings suggest that cortactin is an important component of the receptor-mediated endocytic machinery, where, together with actin and dynamin, it regulates the scission of clathrin pits from the plasma membrane. Thus, cortactin provides a direct link between the dynamic actin cytoskeleton and the membrane pinchase dynamin that supports vesicle formation during receptor-mediated endocytosis.

The actin cytoskeleton, with its associated proteins, has been implicated in endocytic processes in both yeast and mammalian cells (5, 25, 41). How this cytoskeletal network might interact with the endocytic machinery to regulate vesicle formation and scission remains unclear. Recently, Pelkmans and colleagues reported that actin and dynamin accumulated at simian virus 40-docked caveolae concomitant with internalization, thus demonstrating that actin functions during the endocytic process (24). Similarly, Merrifield et al. demonstrated that clathrin, dynamin, and actin are sequentially recruited to form clathrin pits, marked by an accumulation of actin and movement of the vesicles away from the plasma membrane (20). Both of these studies demonstrated an accumulation of dynamin and actin at the forming endocytic membranes but did not directly link the endocytic and cytoskeletal machineries. Recently, it was demonstrated that the actin-binding protein cortactin associates directly with the large GTPase dynamin (Dyn2) via their Src homology three (SH3) and proline-rich domains (PRD), respectively (19). As Dyn2 participates in the liberation of clathrin-coated pits (CCPs) from the plasma membrane, a potential link exists between the endocytic machinery and the actin cytoskeleton through cortactin (18).

Cortactin is an 80- and 85-kDa protein that localizes within membrane ruffles in cultured cells (19, 43) and was originally identified as a substrate for the protein tyrosine kinase pp60Src (21, 44). Importantly, cortactin contains an N-terminal acidic region that, through the three-amino-acid DDW motif, binds to the Arp2/3 complex, where it appears to regulate actin polymerization (36, 39, 40). Cortactin also contains tandem repeats that form F-actin-binding domains (41, 43) and an α-helical proline-rich region that includes tyrosine residues that are phosphorylated by c-Src (12, 13). These unique features make it likely that cortactin participates in numerous actin-dependent cytoskeletal processes. For example, the observations that cortactin is localized to cortical ruffles and that cells expressing high levels of cortactin have enhanced cell motility suggests that cortactin functions together with actin to promote cell motility (23, 43). However, recent studies have reported that cortactin associates with motile endosomes and have implicated this protein in actin nucleation as it may relate to vesicle transport, targeting, or fusion (14, 16, 22, 29). A recent study reporting a direct binding of Dyn2 and cortactin was one of the first to demonstrate a physical interaction between an actin-binding protein and a component of the endocytic machinery (19). Whether cortactin participates in endocytosis is currently undefined.

In this study we tested whether cortactin functions during the initial stages of receptor-mediated endocytosis (RME). Specifically, we asked whether cortactin, normally found at the cell cortex, might also associate with CCPs. Dyn2 mutants that alter RME were used to gain insight into the function and targeting of cortactin to CCPs. The role of cortactin in endocytosis was tested directly through microinjection of affinity-purified antibodies to distinct domains of cortactin, including the dynamin-binding SH3 domain, and by transient expression of the SH3 domain. Multiple endocytic pathways were tested, including the RME uptake of ligands including fluorescently

* Corresponding author. Mailing address: Dept. of Biochemistry and Molecular Biology, 1721 Guggenheim Building, Mayo Clinic, Rochester, MN 55905. Phone: (507) 284-0683. Fax: (507) 284-0762. E-mail: mcniven.mark@mayo.edu.

tagged transferrin and low-density lipoprotein (LDL) or fluid (rhodamine or fluorescein isothiocyanate [FITC]-tagged dextran) by cultured epithelial cells. A striking colocalization of cortactin was observed with both clathrin and Dyn2 puncta on the cell surface by using two distinct cortactin antibodies and red fluorescence protein-tagged cortactin (cortactin-RFP). Further, when RME and clathrin organization was disrupted through the expression of Dyn2 mutant proteins, cortactin redistributed to localize with clathrin in large surface plaques. In support of these findings, microinjection of the same antibodies used for colocalization and expression of the cortactin SH3 domain resulted in a substantial inhibition of clathrin-mediated transferrin and LDL uptake while fluid uptake remained unaffected. These findings demonstrate a role for cortactin at the site of endocytic pit formation and scission.

MATERIALS AND METHODS

Antibodies, ligands, and stains. An anticlathrin monoclonal antibody (X-22) was from the American Type Culture Collection, Rockville, Md. The anti-kinesin (MC44) antibody was raised against a peptide sequence representing amino acids QKKLSGKLYLVDLAGSEKVSKTGAEGT. The anti-cortactin AB3 antibody was raised against the peptide DKSAVGFDYQGKTEKHESQKDYSK, present in the third F-actin-binding domain, and the anti-cortactin C-Tyr antibody was raised against the peptide HYQAEDDTYDGYESDLGIT, present in the C-terminal region of cortactin. The anti-cortactin SH3 antibody was raised against the peptide YDYQAAGDDEISFDPDDVITNIEM, present in the SH3 domain of cortactin. The cortactin antibodies are specific, as confirmed by immunoblotting and immunofluorescence analysis compared to a commercially available monoclonal cortactin antibody 4F11 (Upstate Biotechnology, Lake Placid, N.Y.). Goat anti-rabbit or goat anti-mouse secondary antibodies conjugated to Alexa 488 or 594 were from Molecular Probes (Eugene, Oreg.). Transferrin Alexa 488 or 594, DiI-LDL, and rhodamine- or FITC-dextran (3,000 molecular weight) for immunocytochemical staining were from Molecular Probes. All other chemicals and reagents, unless otherwise stated, were from Sigma (St. Louis, Mo.).

Dynamin and cortactin cDNAs. The Dyn2 (aa) K44A-GFP and Dyn2 (amino acid) ΔPRD-GFP plasmids were as described previously (3, 19). Oligonucleotide primers specific for cortactin were designed (MacVector or Oligo, version 6.51) and synthesized (Applied Biosystems model 394 DNA/RNA synthesizer) by using the cortactin cDNA sequence from GenBank (accession no. AF054619). Primers designed for cortactin are Cort 5′ (ATGTGGAAAGCCTCTGCAGG CCATGCTGTG) and Cort 3′, (CTACTGCCGCAGC TCCACATAG). Full-length cDNAs were amplified by using the XL PCR kit (Perkin Elmer, Branchburg, N.J.). The PCR cycle conditions were 94°C for 1 min and 62°C for 5 min for 28 cycles followed by 72°C for 7 min. The cortactin SH3 domain was amplified by using a PCR kit (Invitrogen, Carlsbad, Calif.). Primers designed for the cortactin SH3 domain were SH3-5′ (ATGTATGACTACCAGGCTGCTGGCG ATG) and the 3′ primer Cort 3′. The cortactin full-length DNA template was used in the PCR; cycle conditions were as described above for 30 cycles. The PCR fragments were ligated into the eukaryotic expression vector pCR3.1 (Invitrogen). For subcloning, positive pCR3.1 subclones were subjected to PCR with 5′ and 3′ PCR primers for cortactin that introduced novel restriction enzyme sites (*Eco*RI and *Bam*HI). Amplification products containing the *Eco*RI and *Bam*HI restriction sites were digested and subcloned into the pDsRed-N_1 (RFP) expression vector (Clontech, Palo Alto, Calif.). Restriction enzymes were from Promega (Madison, Wis.) and Life Technologies, Inc. (Invitrogen).

Cell culture and transfection. Clone 9 cells, an epithelial cell line isolated from normal rat liver (ATCC CRL-1439), were maintained in Ham's F-12K medium supplemented with 10% fetal bovine serum (Invitrogen), 100 U of penicillin/ml, and 100 μg of streptomycin/ml in 5% CO_2–95% air at 37°C. Cells were cultured in T-75 flasks (Fisher Scientific, Pittsburgh, Pa.) or on 22- by 22-mm glass coverslips for transfections and immunocytochemistry, respectively. Transfections were performed with the Lipofectamine Plus reagent kit (Invitrogen).

Immunofluorescence and confocal microscopy. For immunofluorescence microscopy and confocal microscopy, cells were grown on coverslips for 1 to 2 days and prepared as described previously (2). Clone 9 cells were double stained with anti-cortactin (AB3) polyclonal antibody or anti-cortactin (C-Tyr) polyclonal antibody with clathrin (X-22) monoclonal antibody. Transiently transfected cortactin-RFP-expressing cells were also costained with clathrin (X-22). The anti-cortactin and anti-SH3 antibodies were used to identify the Cort SH3-pCR3.1-expressing cells. For the transferrin uptake experiments, the cells were permeabilized with 0.01% digitonin (Fluka, Ronkonkoma, N.Y.). Cells were viewed with an Axiovert 35 epifluorescence microscope (Carl Zeiss, Inc., Thornwood, N.Y.) equipped with a 100-W mercury lamp and a 100× objective lens (Zeiss Plan-Neofluar 1.30) and a confocal microscope (LSM-310 or 510; Carl Zeiss, Inc.) equipped with an argon–krypton laser and a 100× objective lens.

Electron microscopy. Electron microscopy of replica coated, unroofed COS7 cells and labeling with anti-cortactin antibodies were performed as described previously by J. Heuser (9, 10).

Microinjection of anti-cortactin and kinesin antibodies and endocytic assays. Clone 9 cells were microinjected with either buffer alone (10 mM KH_2PO_4 [pH 7.2] and 75 mM KCl) or buffer containing cortactin (AB3, 6.2 mg/ml), cortactin (C-Tyr, 9.4 mg/ml), or anti-kinesin (7.2 mg/ml) antibodies, respectively. Fixable rhodamine- or FITC-dextrans were included in the injectate to identify the injected cells. The cells recovered in 5% CO_2–95% air at 37°C for 4 to 6 h prior to the endocytic assays (8).

Quantitation of transferrin, LDL, and dextran uptake in microinjected cells. Images for quantitation were acquired by using a cooled charge-coupled device camera (Photometrics SenSys, Tuscon, Ariz.) driven by Metamorph (Universal Imaging, West Chester, Pa.). All images of microinjected cells were taken at full resolution (1,024 by 1,024 pixels) with the same acquisition settings (exposure time, 5 s; 12-bit grayscale). The percentage of cells demonstrating an inhibition of transferrin or dextran uptake was determined by visual inspection. The mean percentage of cells showing reduced internalization was determined from three separate experiments and at least 150 cells for each condition. Fluorescence intensity quantitation was performed with IPLab (Scanalytics, Inc., Fairfax, Va.). The area occupied by each cell was traced, and the mean fluorescence intensity per unit area was determined for at least 100 cells in each injection condition.

RESULTS

Cortactin localizes to CCPs in cultured cells. As novel cortactin antibodies were generated for this study, we first needed to demonstrate their specificity. Polyclonal antibodies against cortactin peptides were raised to distinct epitopes in cortactin, the third actin-binding motif (AB3) near the center of the protein, and a C-terminal region adjacent to the SH3 domain known to contain several Src-phosphorylated tyrosines (C-Tyr) (Fig. 1a) (12, 13). After purification and concentration, these antibodies were characterized by using multiple criteria and their specificities were compared to a commercially available cortactin monoclonal antibody (see Materials and Methods). First, immunoblotting of liver homogenate, cultured rat hepatocyte (clone 9) lysate, and purified His_6-cortactin protein demonstrated that all three antibodies specifically detected the characteristic cortactin doublet at 80 and 85 kDa (Fig. 1b). Next, we used these three antibodies to immunoprecipitate cortactin from clone 9 lysate. Immunoblotting of the respective immunoprecipitations with the monoclonal antibody revealed that a substantial amount of cortactin was isolated (Fig. 1c). Importantly, when these immunoprecipitations were subjected to Coomassie blue staining (silver staining was also performed) (data not shown), cortactin represented the overwhelming majority of the protein present (Fig. 1d). These experiments demonstrated that the three distinct antibody reagents used in this study are specific for cortactin.

To define the localization and function of cortactin in cultured clone cells, the purified cortactin antibodies were used for indirect immunofluorescence staining (Fig. 2a and b). Both antibodies gave nearly identical staining patterns, stained the cell cortex, as reported previously (19, 40, 43), and also labeled prominent, punctate foci along the cell surface. Costaining of these cells with monoclonal antibodies to the clathrin heavy chain, or Dyn2 (data not shown), demonstrated a striking, but not absolute, colocalization of these proteins at plasma mem-

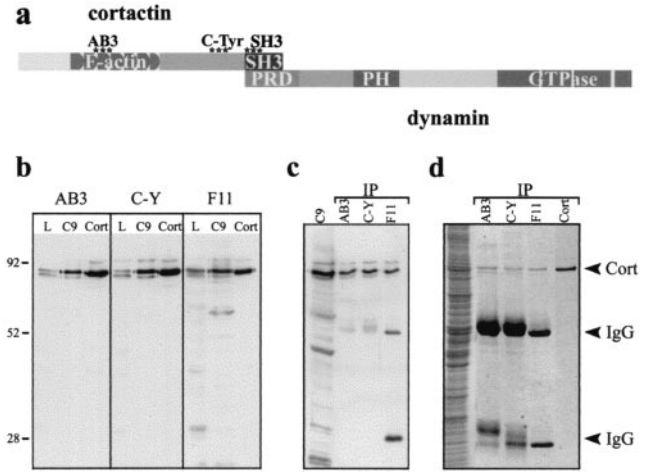

FIG. 1. Polyclonal antibodies raised against distinct cortactin peptides appear specific for the cortactin protein. (a) The diagram depicts different domains of the cortactin protein including the F-actin-binding sites, C-terminal tyrosines that are phosphorylated by Src kinases, and the SH3 domain that binds Dyn2. Areas that peptide antibodies were directed against are indicated (asterisks). To test the specificity of the antibodies, peptide affinity-purified serum was used for immunoblotting and immunoprecipitation. (b) An equal mass of total lysate from rat liver homogenate, cultured hepatocyte (clone 9 [C9]) lysate, or purified His_6-cortactin (Cort) were immunoblotted with either the AB3, C-Tyr (C-Y), or a commercially available cortactin monoclonal antibody (4F11 [F11]; Upstate Biotechnology). The polyclonal anti-cortactin antibodies and the 4F11 antibody specifically detected cortactin in all conditions. (c) Cortactin was immunoprecipitated (IP) from clone 9 lysates with each antibody, and the precipitated protein was immunoblotted with the 4F11 antibody. All cortactin antibodies tested precipitated cortactin that was easily detected by immunoblotting. (d) Coomassie staining of the immunoprecipitation reactions demonstrated that a substantial amount of cortactin was obtained and that it was the major protein species present (compare the bands from the immunoprecipitations against 0.2 μg of purified His_6-cortactin [Cort]). IgG, immunoglobulin G.

brane puncta (Fig. 2a to b″). To further confirm these antibody localization results, clone 9 cells expressing a cortactin-RFP fusion protein (Cort-B-pDsRed-N_1) were fixed and stained with antibodies to clathrin (Fig. 2c to c″) or Dyn2 (data not shown). As for the antibody-stained cells, the expressed cortactin-RFP localized to the cell cortices and in small puncta along the cell surface that stained positive for both clathrin and Dyn2. A majority, but not all, of the tagged cortactin protein associated with clathrin foci (Fig. 2c″).

To visualize cortactin's localization at the ultrastructural level and gain insight into its potential function at CCPs, unroofed preparations of cultured COS7 cells were processed for immuno-gold electron microscopy with the AB3 or C-Tyr cortactin antibodies by using the methods of Heuser (9, 10). This preparation allows high-resolution imaging of immuno-gold complexes while maintaining remarkable morphological preservation of coat and cytoskeletal components along the cell cortex at the plasma membrane. In support of the fluorescence microscopy images shown in Fig. 2a to c″, the immuno-gold electron microscopy wtih cortactin antibodies revealed a strong labeling of both flat and highly curved clathrin lattices (Fig. 2d to f). Interestingly, gold particles appeared to be distributed randomly over the surface of flat clathrin lattices, but this distribution became restricted to a ring around the base of the clathrin coat as the pit invaginated (Fig. 2d versus e and f). This circular distribution along the base of protruding pits closely resembled that of Dyn2 as viewed in the same preparation (data not shown). Importantly, the cortactin antibodies also labeled actin filaments in these preparations (Fig. 2d to e). Thus, two different purified antibodies directed to distinct motifs in the cortactin protein, as well as cortactin-RFP, showed significant localization, with CCPs at both the light and ultrastructural levels. These morphological findings strongly supported a potential role for cortactin in RME together with actin and dynamin.

To further confirm that cortactin is a component of CCPs and to elucidate the role of cortactin together with Dyn2 at CCPs, we disrupted the normal punctate distribution of clathrin in cultured cells via expression of mutant Dyn2 proteins. The GTP-binding and hydrolysis-deficient Dyn2K44A is often used to block RME, and its expression is proposed to block pits at the intermediate stage of internalization, prior to final constriction of the vesicle neck (4, 11, 37). Dynamin that lacks the PRD, Dyn2ΔPRD, has a diffuse, largely cytoplasmic staining pattern, cannot bind to cortactin (19), and was recently shown not to target to CCPs, resulting in blocked RME (32). Dyn2ΔPRD is proposed to exert its dominant-negative effect by inappropriately targeting in cells and through oligomerization with endogenous dynamin (19, 32). Interestingly, when Dyn2K44A- or Dyn2ΔPRD-expressing cells (data not shown) were stained for cortactin and clathrin, the distribution of plasma membrane cortactin changed to become part of the large, abnormal clathrin aggregates (Fig. 3). The fact that cortactin localization changed along with CCP formation and distribution supports the morphological observations shown in Fig. 2, indicating that the actin-binding protein cortactin is part of the clathrin endocytic machinery.

Cortactin, including its SH3 domain, is important for efficient RME. To directly test the role of cortactin in endocytosis, the same affinity-purified antibodies used to show a localization of cortactin to CCPs (Fig. 2) were microinjected into clone 9 cells. First, we demonstrated that the injected cells did not display any gross morphological defects compared to noninjected, buffer-injected, or kinesin antibody-injected cells (Fig. 4 and data not shown). This suggested that the cells were healthy in the context of these experiments. Based on cortactin's localization to CCPs, we expected that an antibody-mediated inhibition of cortactin function could have profound effects on RME. To test if the cortactin antibodies that colocalize with CCPs might affect clathrin-mediated endocytosis of transferrin or LDL or fluid-phase endocytosis of dextran, cells were injected with control solutions (microinjection buffer alone or a kinesin antibody) or affinity-purified cortactin antibodies. Injected cells recovered for 4 h prior to incubation with fluorescent ligands. Subsequent to rinsing and fixation, cells were scored in a blind fashion as normal or significantly inhibited for endocytosis. While buffer alone (data not shown) or the purified kinesin antibody had no effect on transferrin uptake (Fig. 4a), both the cortactin AB3 and C-Tyr antibodies exhibited a profound inhibitory effect on ligand uptake (Fig. 4b and c). In over 80% (AB3-injected) and 70% (C-Tyr-injected) of the cells counted, transferrin internalization appeared completely ablated (Fig. 4e). Interestingly, while transferrin staining in con-

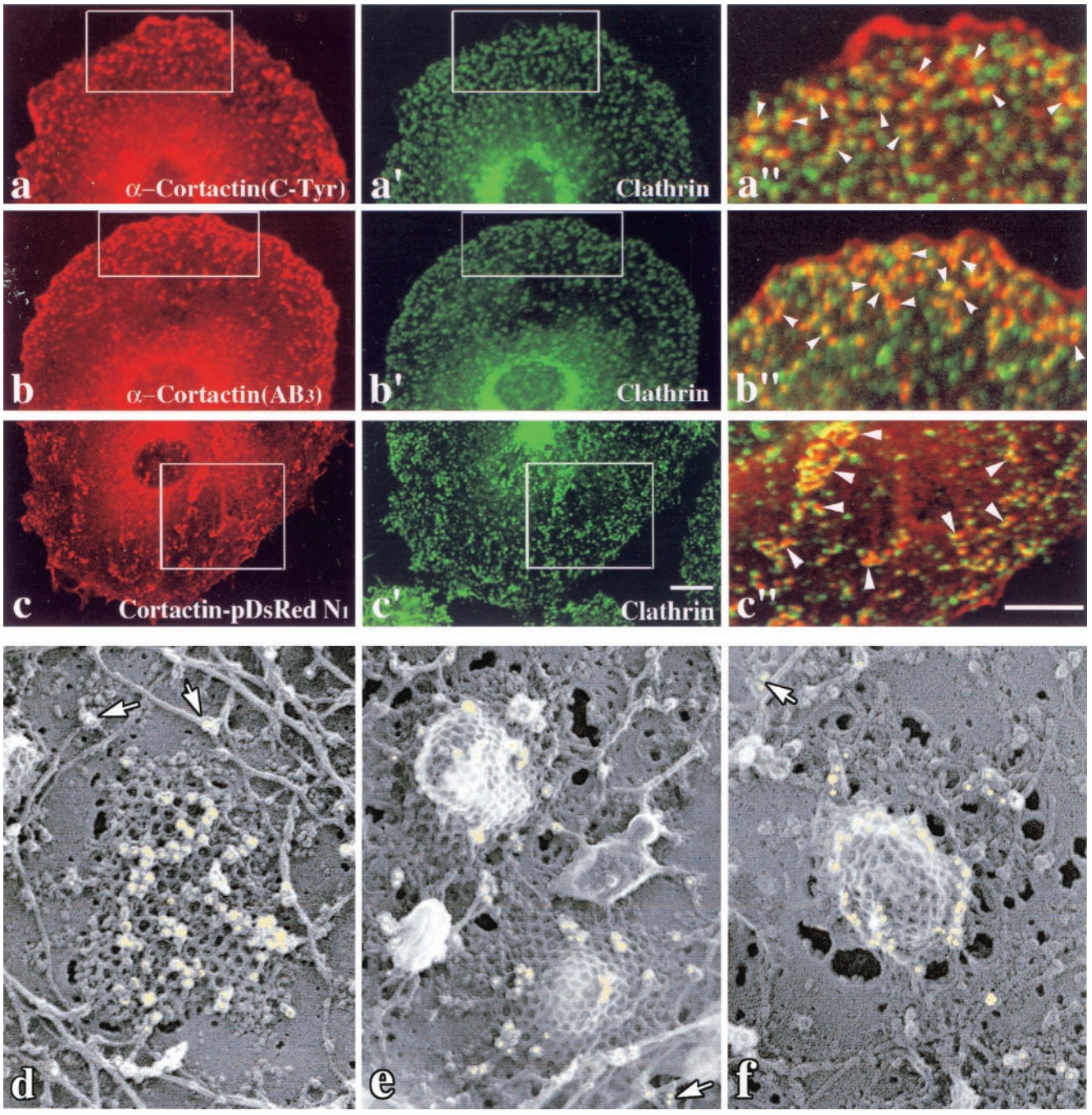

FIG. 2. Cortactin antibodies stain numerous plasma membrane foci that colocalize with CCPs. (a to c″) Immunofluorescence microscopy of cultured clone 9 cells stained with cortactin antibodies directed to the C-Tyr (a) and the actin-binding (AB3) (b) domains. Both antibodies labeled small punctate foci on the basal plasma membrane that colocalize significantly (arrows) with clathrin (a″ and b″). Fluorescence images of clone 9 cells expressing cortactin-RFP and costained for clathrin are shown (c to c″). As for the antibody staining, significant levels of the tagged cortactin protein associated with numerous punctate foci along the ventral membrane. (c″) Higher-magnification images of the boxed regions show that a substantial number of the cortactin-RFP- and clathrin-positive puncta overlap or are in close association. (d to f) Immunoelectron microscopy of the inner plasma membrane of unroofed COS7 cells labeled with the C-Tyr (d and e) and AB3 (f) cortactin antibodies. Flat or curved clathrin lattices as well as actin filaments can be seen associated with the plasma membrane. Numerous immuno-gold particles (yellow) can be seen specifically labeling the clathrin cage and appear to cluster in a concentric ring along the pit base, as opposed to the bulb, as the membrane invaginates (g). (d to f) Gold particles can also be resolved on actin filaments and actin filament branches (arrows). Bars = 10 μm (a to c″). Magnification, ×72,750 (d to f).

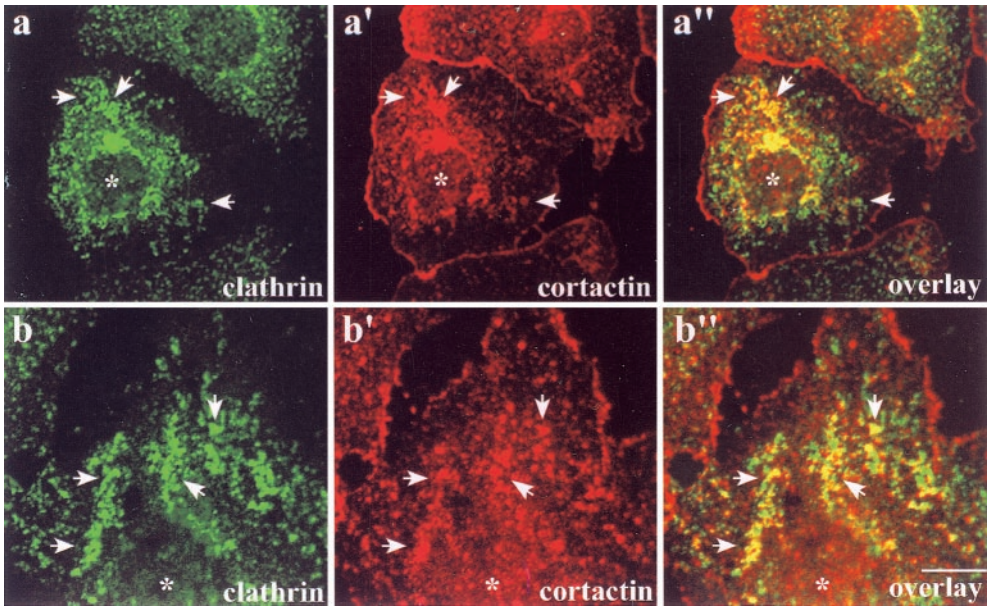

FIG. 3. Inhibition of clathrin-mediated endocytosis in cells expressing GTPase-deficient Dyn2 results in an abnormal distribution of both cortactin and clathrin. Clone 9 cells transiently expressing GTPase-deficient Dyn2K44A-GFP were fixed and labeled to visualize the clathrin (X-22 monoclonal antibody) and cortactin (C-Tyr). (a to a″) Cells expressing the Dyn2 mutant (asterisks) have numerous clustered and clumpy-looking clathrin pits (a′ and b′, arrows) in comparison to neighboring nontransfected cells. The defective clathrin staining dramatically colocalized with cortactin (a″ and b″, arrows). Bar = 10 μm.

trol cells was distributed as clustered small puncta near the nucleus and plasma membrane, some cortactin antibody-injected cells (20 to 30%) displayed a substantial, but not complete, decrease in staining intensity at both locations (data not shown). Thus, we elected to digitally quantify the mean fluorescence intensity per unit area of internalized transferrin in these inhibited cells. While microinjection of buffer alone or kinesin antibody did not result in decreased transferrin intensity, the cortactin antibody-injected cells that showed partial inhibition were on average only 40% as intense as control, noninjected cells (Fig. 4f). Consistent with the transferrin internalization experiments, the RME of LDL was also affected. Microinjection of the same cortactin antibodies resulted in a block of LDL internalization in the majority of cells (Fig. 5a, a′, and c). Upon quantitation of the mean fluorescence intensity of LDL in these cells, there was a 40 to 50% decrease in internalization compared to control (Fig. 5d). These results, together with the cells that appeared to be completely blocked in each condition, indicated that the cortactin antibodies potently inhibited the internalization of transferrin and LDL. In contrast, cortactin antibody-injected cells showed no reduction in the ability to internalize fluid markers, such as fluorescent dextran (Fig. 6).

In an attempt to further define how cortactin may mediate RME, we transiently expressed the cortactin SH3 domain in cells. We rationalized that the expressed SH3 domain could competitively inhibit RME by interfering with the normal function of cortactin and interactions with its binding partners, such as dynamin. Mainly, expression of the SH3 domain produced cell phenotypes strikingly similar to those observed in the antibody microinjection experiments and significantly reduced the uptake of transferrin (Fig. 4d, e, and g), and LDL (Fig. 5b, b′, e, and f). Importantly, expression of full-length cortactin in these same experiments had no significant effects on RME (Fig. 4e and g and 5e and f). These results suggested that the SH3 domain of cortactin has an important role in linking cortactin and/or dynamin to the functional endocytic complex.

DISCUSSION

In this study we demonstrate a structural and functional association between the actin-binding protein cortactin and CCPs in cultured epithelial cells. This study was initiated based on previously published data that the SH3 domain of cortactin binds to the proline-rich tail of Dyn2 (19). While this earlier study demonstrated a convincing codistribution of these proteins in peripheral membrane ruffles, it was unclear if an association occurred at the site of RME. Because dynamin functions during the endocytic process, it prompted us to test if cortactin and Dyn2 interactions are required to support invagination of the plasma membrane and subsequent internalization of ligand. Several morphological techniques demonstrated a convincing colocalization between cortactin, Dyn2, and clathrin. The methods used in this study included immunofluorescence cell staining with two polyclonal antibodies made to distinct cortactin domains (Fig. 2), expression of RFP-tagged cortactin protein (Fig. 2), and high-resolution immuno-gold electron microscopy with the same antibodies (Fig. 2). All three of these methods were supportive of each other and consistently localized cortactin to CCPs. Interestingly, the electron micrographs showed that at initial steps of invagination, cortactin localized throughout flat clathrin lattices. At later stages, the cortactin was primarily located in a ring or collar around the neck of the pit, with some occasionally remaining at

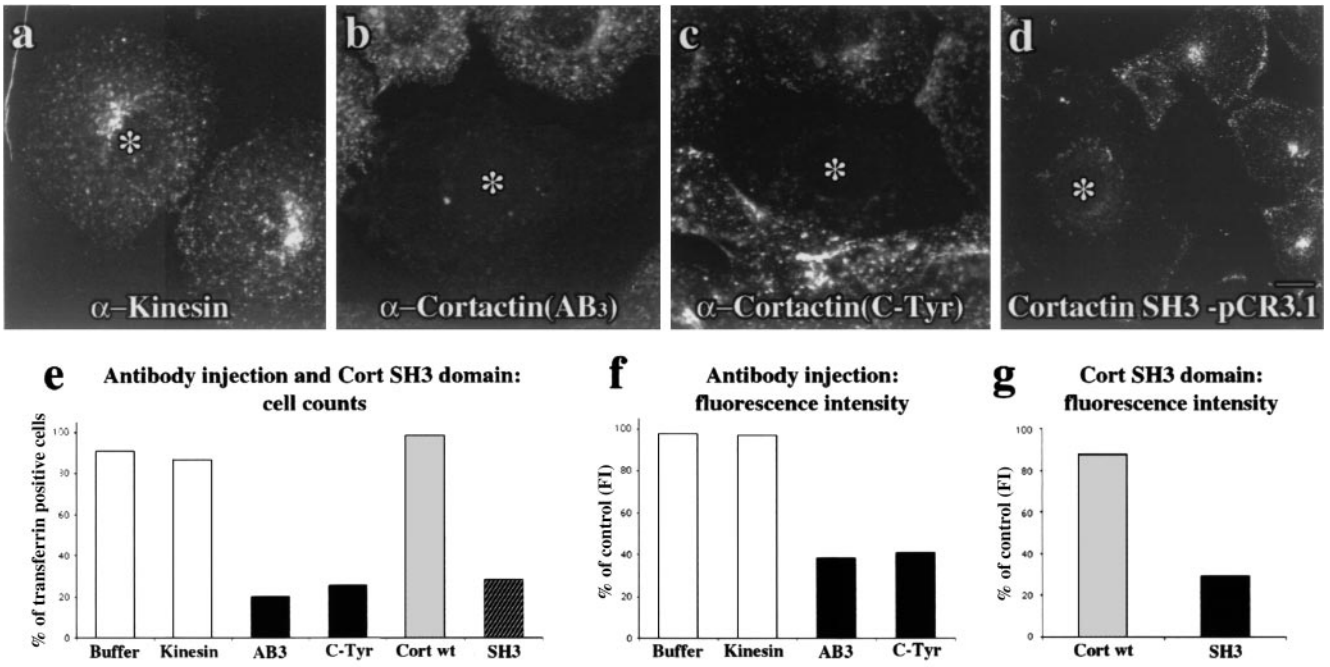

FIG. 4. Cortactin antibody injection and expression of the SH3 domain significantly inhibit RME of transferrin. (a) Transferrin fluorescence images of cultured cells microinjected (asterisk) with purified antibodies or expressing the cortactin SH3 domain. All injectate solutions contained FITC-dextran to confirm successful injections. Injection of kinesin antibody had no effect on the internalization of Alexa 594-transferrin. (b and c) In contrast, cells microinjected with either the AB3 or C-Tyr purified cortactin antibodies showed significant inhibition of the RME of Alexa 594-transferrin. (d) Expression of the SH3 domain also potently blocked transferrin internalization, demonstrating the importance of cortactin's SH3 domain for RME. Bar = 10 μm. (e) The antibody-injected and SH3 domain-expressing cells showing a block in endocytosis were counted. Whereas the number of cells with normal uptake is not affected in buffer and kinesin antibody-injected cells, only ~20% of cells injected with cortactin antibody or expressing the SH3 domain had normal uptake. (f and g) Fluorescence intensity (FI) quantitation of internalized transferrin confirmed that, when compared to controls, there is a significant 60% block in the antibody-injected cells (f) and a 70% block in the cells expressing the SH3 domain (g). Cort wt = full-length cortactin, SH3 = cortactin SH3 domain.

the bulb of the invaginating pit. This is not unlike what we and others have observed for dynamin (4, 33). Exactly why some of the cortactin and Dyn2 remain associated with the bulb of the pit is unclear, but perhaps part of this complex is a remnant of the protein associated with the flat clathrin lattice prior to curvature or is providing nucleation sites for actin filaments to push the vesicle from the plasma membrane.

Consistent with the localization studies, the same antibody reagents exhibited a potent inhibitory effect on cell function. Both antibodies significantly inhibited RME of transferrin and LDL but not the uptake of fluid markers (Fig. 4, 5, and 6). As multiple laboratories have observed different requirements for dynamin in fluid-phase internalization (6, 16, 22), it was unclear if cortactin would be required in this process or not. One possibility is that cortactin's role in fluid-phase endocytosis is not during internalization but rather during postendocytic trafficking and movement via actin polymerization, as has been observed for both cortactin and Dyn2 (14, 16, 22). It is likely that cortactin is associated with actin microfilaments in close proximity to the clathrin lattice (Fig. 2d to f). Actin microfilaments are thought to function during early stages of pit invagination and to organize pit assemblies that aid in nascent vesicle fission from the plasma membrane (26, 28). Cortactin's proposed function as a protein that enhances microfilament nucleation via the Arp2/3 complex and stabilizes actin filaments and branches supports such a function for cortactin in RME. Further, recent data demonstrating cortactin's role together with Dyn2 in other actin-dependent membrane processes supports the hypothesis that cortactin and Dyn2 function together with actin to mediate vesicle formation. The action of such a complex could be coordinated by integration with a host of proteins. The Dyn2 polymer, along with cortactin, could form a complex meshwork comprised of multiple actin-binding proteins including profilin (42), Abp1 (15), syndapin (25), N-WASp (35); structural coat proteins such as amphiphysin (7), AP2 (38), and clathrin (34); and signaling molecules including PIP2 (17, 45), phospholipase C-γ (31), and Src (1, 5). The cortactin SH3 domain expression experiments demonstrate that the SH3 domain of cortactin is important for RME. It is attractive to predict that cortactin's SH3 domain is binding to dynamin and other putative partners at the forming vesicle. As the injection of cortactin antibodies or expression of multiple truncated cortactin constructs did not inhibit the recruitment of Dyn2 to clathrin pits, it is likely that cortactin does not directly recruit Dyn2 to the pit. As there are multiple Dyn2-binding partners at the endocytic site (endophilin, intersectin, amphiphysin, Grb2, and AP2) (18), it is likely that the Dyn2-cortactin binding contributes to membrane deformation and actin assembly rather than direct recruitment.

Finally, dynamin is known to interact with other actin-associated proteins, including syndapin (27), profilin (42), and Abp1 (15). Abp1 was shown to regulate RME through actin

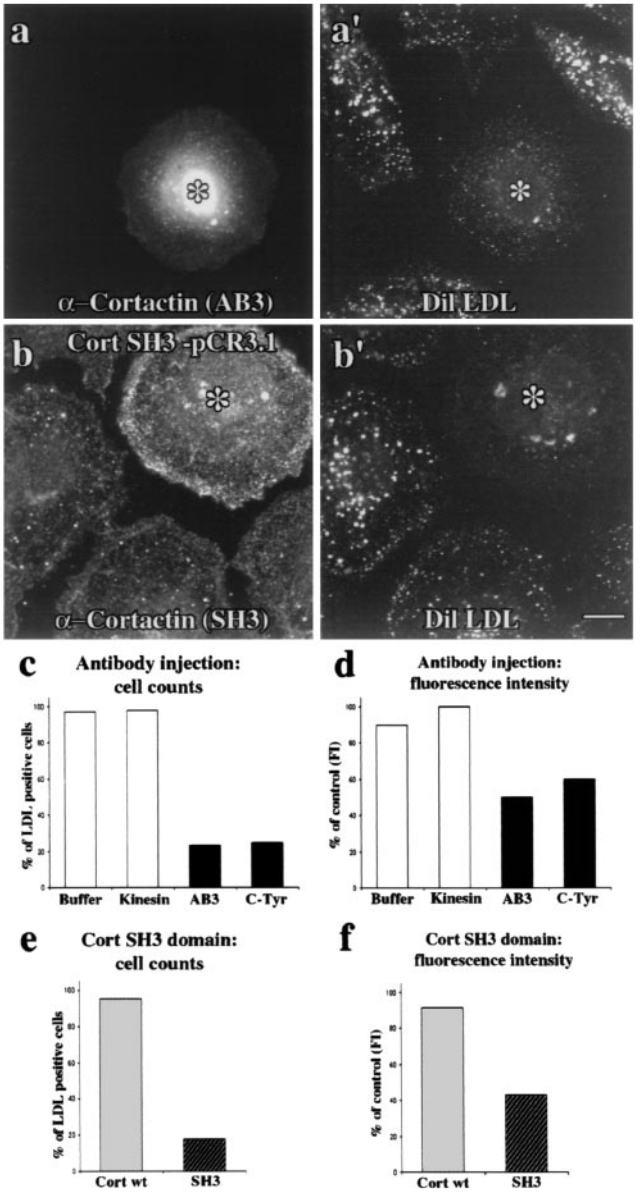

FIG. 5. Cortactin function is also required for the RME of LDL. (a and a′) A cortactin AB3 antibody-injected cell (asterisk) demonstrating a significant block in the level of internalized DiI-LDL compared to neighboring noninjected cells. (b and b′) Cells expressing the cortactin SH3 domain (asterisk) also demonstrated substantially reduced internalization of LDL compared to neighboring, nonexpressing cells. (c and d) Quantitation of the effect of cortactin antibody injection on LDL internalization. Nearly 80% of the cells injected with cortactin antibodies appeared blocked. Fluorescence intensity (FI) quantitation of internalized LDL in these antibody-injected cells showed only 40 to 50% uptake compared to buffer-injected, kinesin antibody-injected, or noninjected neighbors. (e and f) Quantitation of the effect of cortactin SH3 domain expression on LDL internalization. Over 80% of the cells expressing the SH3 domain appeared blocked (e). Fluorescence intensity quantitation of internalized LDL in these SH3 domain-expressing cells showed only 40 to 50% uptake compared to neighboring nontransfected cells (f). Bar = 10 μm. Cort wt, full-length cortactin; SH3, cortactin SH3 domain.

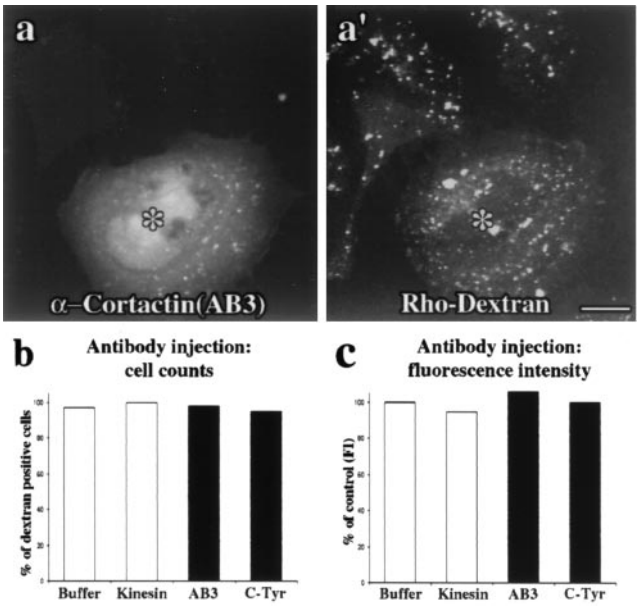

FIG. 6. Inhibition of cortactin does not significantly affect fluid-phase endocytosis. (a and a′) Cortactin antibody (AB3)-injected cells (FITC-dextran) (asterisks) showed no obvious defect in the internalization of rhodamine-labeled dextran compared to their noninjected neighbors. (b) The number of cells with normal uptake was unaffected in cortactin antibody-injected cells, as reflected by the same number of dextran-positive cells compared to buffer- and kinesin antibody-injected cells. (c) In agreement with the immunocytochemistry experiments, quantitation of the mean dextran fluorescence intensity (FI) per unit area in cortactin antibody-injected cells revealed no significant difference in dextran uptake compared to control conditions. The results in this figure suggest that the reagents used in this study specifically affect cortactin function during RME and not during fluid-phase endocytosis. Bar = 10 μm.

and dynamin (15). Significantly, mammalian Abp1, unlike cortactin, lacks the acidic amino acid residues that mediate direct binding to the Arp2/3 complex (28). This is an important distinction that increases the inherent importance of the cortactin-Dyn2 interaction. Actin nucleation has been suggested to be important for RME, and the fact that cortactin stimulates actin nucleation and that this activity is affected by binding to dynamin (30) suggests that cortactin may serve a more direct role during RME, rather than functioning as a scaffolding molecule that links actin filaments and Dyn2. Interestingly, when cortactin's binding domain is removed from Dyn2 (Dyn2ΔPRD), there are alterations in associated actin organization, Dyn2 no longer localizes to CCPs and RME is inhibited (19, 22, 32). Based on this study, and others, an attractive model predicts that the SH3 domain of cortactin binds to the PRD of Dyn2 at the invaginating CCP. The direct interaction of these two proteins integrates dynamic actin filaments and the membrane fission machinery, possibly in a Src-sensitive manner. Thus, the actin filament-binding and nucleation activity of cortactin and the membrane-modeling activity of Dyn2 may function together during RME to mediate the final scission step of endocytosis. A simplified model depicting cortactin and dynamin and how they may integrate endocytic proteins at the invaginating pit is shown in Fig. 7. Future studies further defining how cortactin and Dyn2 mediate membrane invagina-

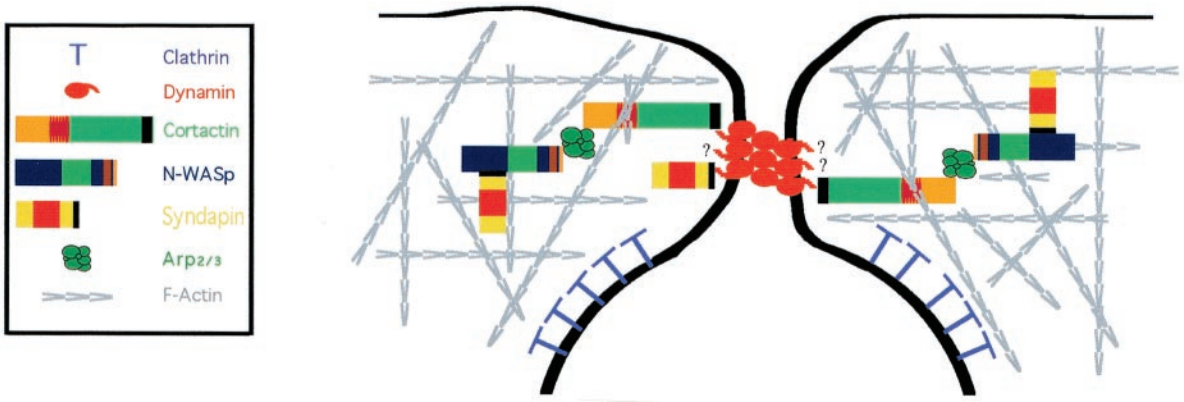

FIG. 7. Dynamin and cortactin as key components of the cytoskeletal-endocytic machinery. Dynamin interacts with numerous proteins that function to regulate clathrin-dependent endocytosis. Oligomers of dynamin function to restrict or pinch the neck of the invaginating membrane while multiple extended PRDs interact directly with a variety of other proteins, including cortactin, that serve to link Dyn2 to the actin cytoskeleton and the Arp2/3 complex. The complex cytoskeletal network also includes interactions with other actin-binding proteins such as syndapin, N-WASp, Abp1, and Hip1R (some not shown for simplification).

tion will provide important insights into the regulation of the endocytic process.

ACKNOWLEDGMENTS

We thank H. M. Thompson for critical reading of the manuscript.

This study was supported by funding to M.A.M. from the NIH and Mayo Foundation.

REFERENCES

1. **Ahn, S., S. Maudsley, L. M. Luttrell, R. J. Lefkowitz, and Y. Daaka.** 1999. Src-mediated tyrosine phosphorylation of dynamin is required for beta2-adrenergic receptor internalization and mitogen-activated protein kinase signaling. J. Biol. Chem. **274:**1185–1188.
2. **Cao, H., F. Garcia, and M. McNiven.** 1998. Differential distribution of dynamin isoforms in mammalian cells. Mol. Biol. Cell **9:**2595–2609.
3. **Cao, H., H. M. Thompson, E. W. Krueger, and M. A. McNiven.** 2000. Disruption of Golgi structure and function in mammalian cells expressing a mutant dynamin. J. Cell Sci. **113:**1993–2002.
4. **Damke, H., D. D. Binns, H. Ueda, S. L. Schmid, and T. Baba.** 2001. Dynamin GTPase domain mutants block endocytic vesicle formation at morphologically distinct stages. Mol. Biol. Cell **12:**2578–2589.
5. **Foster-Barber, A., and J. M. Bishop.** 1998. Src interacts with dynamin and synapsin in neuronal cells. Proc. Natl. Acad. Sci. USA **95:**4673–4677.
6. **Gold, E. S., D. M. Underhill, N. S. Morrissette, J. B. Guo, M. A. McNiven, and A. Aderem.** 1999. Dynamin 2 is required for phagocytosis in macrophages. J. Exp. Med. **190:**1849–1856.
7. **Grabs, D., V. I. Slepnev, Z. Songyang, C. David, M. Lynch, L. C. Cantley, and P. De Camilli.** 1997. The SH3 domain of amphiphysin binds the proline-rich domain of dynamin at a single site that defines a new SH3 binding consensus sequence. J. Biol. Chem. **272:**13419–13425.
8. **Henley, J. R., E. W. Krueger, B. J. Oswald, and M. A. McNiven.** 1998. Dynamin-mediated internalization of caveolae. J. Cell Biol. **141:**85–99.
9. **Heuser, J.** 1989. Changes in lysosome shape and distribution correlated with changes in cytoplasmic pH. J. Cell Biol. **108:**855–864.
10. **Heuser, J. E.** 2000. Membrane traffic in anaglyph stereo. Traffic **1:**35–37.
11. **Hill, E., J. van der Kaay, C. P. Downes, and E. Smythe.** 2001. The role of dynamin and its binding partners in coated pit invagination and scission. J. Cell Biol. **152:**309–323.
12. **Huang, C., J. Liu, C. C. Haudenschild, and X. Zhan.** 1998. The role of tyrosine phosphorylation of cortactin in the locomotion of endothelial cells. J. Biol. Chem. **273:**25770–25776.
13. **Huang, C., N. Yansong, T. Wang, Y. Gao, C. C. Haudenschild, and X. Zhan.** 1997. Down-regulation of the filamentous actin cross-linking activity of cortactin by Src-mediated tyrosine phosphorylation. J. Biol. Chem. **272:**13911–13915.
14. **Kaksonen, M., H. B. Peng, and H. Rauvala.** 2000. Association of cortactin with dynamic actin in lamellipodia and on endosomal vesicles. J. Cell Sci. **113:**4421–4426.
15. **Kessels, M. M., A. E. Y. Engqvist-Goldstein, D. G. Drubin, and B. Qualmann.** 2001. Mammalian Abp1, a signal-responsive F-actin-binding protein, links the actin cytoskeleton to endocytosis via the GTPase dynamin. J. Cell Biol. **153:**351–366.
16. **Lee, E., and P. De Camilli.** 2002. Dynamin at actin tails. Proc. Natl. Acad. Sci. USA **99:**161–166.
17. **Lin, H. C., B. Barylko, M. Achiriloaie, and J. P. Albanesi.** 1997. Phosphatidylinositol (4,5)-biphosphate-dependent activation of dynamins I and II lacking the proline/arginine-rich domains. J. Biol. Chem. **272:**25999–26004.
18. **McNiven, M. A., H. Cao, K. R. Pitts, and Y. Yoon.** 2000. Pinching in new places: multiple functions for the dynamin family. Trends Biochem. Sci. **25:**115–120.
19. **McNiven, M. A., L. Kim, E. W. Krueger, J. D. Orth, H. Cao, and T. W. Wong.** 2000. Interactions between dynamin and the actin binding protein cortactin modulate cell shape. J. Cell Biol. **151:**187–198.
20. **Merrifield, C. J., M. E. Feldman, L. Wan, and W. Almers.** 2002. Imaging actin and dynamin recruitment during invagination of single clathrin-coated pits. Nat. Cell Biol. **4:**691–698.
21. **Okamura, H., and M. D. Resh.** 1995. p80/85 cortactin associates with the Src SH2 domain and colocalizes with v-Src in transformed cells. J. Biol. Chem. **270:**26613–26618.
22. **Orth, J. D., E. W. Krueger, H. Cao, and M. A. McNiven.** 2002. The large GTPase dynamin regulates actin comet formation and movement in living cells. Proc. Natl. Acad. Sci. USA **99:**167–172.
23. **Patel, A. S., G. L. Schechter, W. J. Wasilenko, and K. D. Somers.** 1998. Overexpression of EMS1/cortactin in NIH3T3 fibroblasts causes increased cell motility and invasion in vitro. Oncogene **16:**3227–3232.
24. **Pelkmans, L., D. Puntener, and A. Helenius.** 2002. Local actin polymerization and dynamin recruitment in SV40-induced internalization of caveolae. Science **296:**535–539.
25. **Qualmann, B., and R. B. Kelly.** 2000. Syndapin isoforms participate in receptor-mediated endocytosis and actin organization. J. Cell Biol. **148:**1047–1061.
26. **Qualmann, B., M. M. Kessels, and R. B. Kelly.** 2000. Molecular links between endocytosis and the actin cytoskeleton. J. Cell Biol. **150:**F111–F116.
27. **Qualmann, B., J. Roos, P. J. DiGregorio, and R. B. Kelly.** 1999. Syndapin I, a synaptic dynamin-binding protein that associates with the neural Wiskott-Aldrich syndrome protein. Mol. Biol. Cell **10:**501–513.
28. **Schafer, D. A.** 2002. Coupling actin dynamics and membrane dynamics during endocytosis. Curr. Opin. Cell Biol. **14:**76–81.
29. **Schafer, D. A., C. D'Souza-Schorey, and J. A. Cooper.** 2000. Actin assembly at membranes controlled by ARF6. Traffic **1:**892–903.
30. **Schafer, D. A., S. A. Weed, D. Binns, A. V. Karginov, P. J. T., and J. A. Cooper.** 2002. Dynamin 2 and cortactin regulate actin assembly and filament organization. Curr. Biol. **12:**1852–1857.
31. **Seedorf, K., G. Kostka, R. Lammers, P. Baskku, R. Daly, W. H. Burgess, A. M. van der Bliek, J. Schlessinger, and A. Ullrich.** 1994. Dynamin binds to SH3 domains of phospholipase Cγ and GRB-2. J. Biol. Chem. **269:**16009–16014.
32. **Szaszak, M., Z. Gaborik, G. Turu, P. S. McPherson, A. J. L. Clark, K. J. Catt, and L. Hunyady.** 2002. Role of the proline-rich domain of dynamin-2 and its interactions with Src homology 3 domains during endocytosis of the AT_1 angiotensin receptor. J. Biol. Chem. **277:**21650–21656.
33. **Takei, K., P. S. McPherson, S. L. Schmid, and P. De Camilli.** 1995. Tubular membrane invaginations coated by dynamin rings are induced by GTP-γS in nerve terminals. Nature **374:**186–190.
34. **Takei, K., V. I. Slepnev, V. Haucke, and P. De Camilli.** 1999. Functional

partnership between amphiphysin and dynamin in clathrin-mediated endocytosis. Nat. Cell Biol. **1:**33–39.

35. **Taunton, J., B. A. Rowning, M. L. Coughlin, M. Wu, R. T. Moon, T. J. Mitchison, and C. A. Larabell.** 2000. Actin-dependent propulsion of endosomes and lysosomes by recruitment of N-WASP. J. Cell Biol. **148:**519–530.
36. **Uruno, T., J. Liu, P. Zhang, Y. Fan, C. Egile, R. Li, S. C. Mueller, and X. Zhan.** 2001. Activation of Arp2/3 complex-mediated actin polymerization by cortactin. Nat. Cell Biol. **3:**259–265.
37. **van der Bliek, A. M., T. E. Redelmeier, H. Damke, E. J. Tisdale, E. M. Meyerowitz, and S. L. Schmid.** 1993. Mutations in human dynamin block an intermediate stage in coated vesicle formation. J. Cell Biol. **122:**553–563.
38. **Wang, L. H., T. C. Sudhof, and R. G. Anderson.** 1995. The appendage domain of alpha adaptin is a high affinity binding site for dynamin. J. Biol. Chem. **270:**10079–10083.
39. **Weaver, A. M., A. V. Karginov, A. W. Kinley, S. A. Weed, Y. Li, J. T. Parsons, and J. A. Cooper.** 2001. Cortactin promotes and stabilizes Arp2/3-induced actin filament network formation. Curr. Biol. **11:**370–374.
40. **Weed, S. A., A. V. Karginov, D. A. Schafer, A. M. Weaver, A. W. Kinley, J. A. Cooper, and J. T. Parsons.** 2000. Cortactin localization to sites of actin assembly in lamellipodia requires interactions with F-actin and the Arp2/3 complex. J. Cell Biol. **151:**29–40.
41. **Weed, S. A., and J. T. Parsons.** 2001. Cortactin: coupling membrane dynamics to cortical actin assembly. Oncogene **20:**6418–6434.
42. **Witke, W., A. V. Podtelejnikov, A. Di Nardo, J. D. Sutherland, C. B. Gurniak, C. Dott, and M. Mann.** 1998. In mouse brain profilin I and profilin II associate with regulators of the endocytic pathway and actin assembly. EMBO J. **17:**967–976.
43. **Wu, H., and J. T. Parsons.** 1993. Cortactin, an 80/85-kilodalton pp60^{src} substrate, is a filamentous actin-binding protein enriched in the cell cortex. J. Cell Biol. **120:**1417–1426.
44. **Wu, H., A. B. Reynolds, S. B. Kanner, R. R. Vines, and J. T. Parsons.** 1991. Identification of a novel cytoskeleton-associated pp60^{src} substrate. Mol. Cell. Biol. **11:**5113–5124. arsid7952991
45. **Zheng, J., S. M. Cahill, M. A. Lemmon, D. Fushman, J. Schlessinger, and D. Cowburn.** 1996. Identification of the binding site for acidic phospholipids on the PH domain of dynamin: implications for stimulation of GTPase activity. J. Mol. Biol. **255:**14–21.